Adaptive OFDM Radar for Detecting a Moving Target in Urban Scenarios

Satyabrata Sen, Martin Hurtado, and Arye Nehorai, *Fellow, IEEE*
Department of Electrical and Systems Engineering
Washington University in St. Louis
One Brookings Drive, St. Louis, MO 63130, USA
Email: {ssen3, nehorai}@ese.wustl.edu
Phone: 314-935-7520 Fax: 314-935-7500

***Abstract*—We address the problem of detecting a moving target in an urban canyon using an orthogonal frequency division multiplexing (OFDM) radar and exploiting the multipath reflections. The multipath propagation increases the spatial diversity of the radar system and provides different Doppler shifts over different path. In addition, the use of broadband OFDM signal provides frequency diversity to the system. We develop a parametric measurement model that accounts for the multipath components at multiple frequencies as well as Doppler shifts. Then, we develop a statistical detection test and evaluate its performance characteristics. Based on this, we propose an algorithm to optimally design the spectral weights for the next transmitting waveform. We present a few numerical examples to illustrate our analytical results. We demonstrate the achieved performance improvement due to the exploitation of multipath propagation, OFDM signalling, and adaptive waveform design.**

I. Introduction

Detection and tracking of ground targets in urban environments are becoming increasingly important in defense applications. The urban scenario is rich in multipath propagation generated by multiple reflections, refractions, and scattering of the radar signal from buildings and other structures. In addition, the line-of-sight (LOS) propagation path from the radar to the target may not be available most of the time. Hence, conventional radar systems, which are designed to operate mainly in open environments [1], encounter difficulties in the urban operations. We propose to exploit the multipath reflections rather than canceling them to improve the target-detection performance.

In the urban environments, the building walls produce specular reflections of the radar signal, which impinge on the target from different incident angles. Thus, multipath propagation increases the spatial diversity of the radar system. Furthermore, each multipath component is affected by a different Doppler shift corresponding to the projection of the target velocity on the direction-of-arrival (DOA) vector. Exploitation of multiple Doppler shifts should increase the ability of the radar to detect targets, particularly when the target moves perpendicularly to the radar LOS.

This work was supported by the Department of Defense under the Air Force Office of Scientific Research MURI Grant FA9550-05-1-0443 and ONR Grant N000140810849.

Additionally, we consider a broadband radar transmitting orthogonal frequency division multiplexing (OFDM) signals [2]. The broadband signal mitigates possible fading and resolves the different multipath signals. The frequency diversity of OFDM provides additional information as different scattering centers of a target resonate at different frequencies. Although OFDM has been elaborately studied and commercialized in digital communication field [3], apart from a few recent efforts [4], [5], it has not yet so widely been studied by the radar community.

First, we develop the measurement model that accounts for the multipath components generated by the specular reflections as well as Doppler shifts in Section II. For simplicity we consider only first-order reflections. Then, in Section III, we formulate the detection problem as a hypothesis test to decide about the presence of a moving target. We employ the generalized likelihood ratio (GLR) test to solve this detection problem. Based on the asymptotic performance analysis of our test, in Section IV, we propose an algorithm for adaptively computing the parameters for the next transmitting waveform. To illustrate the potential of our method, we present numerical examples in Section V. Our results demonstrate the achieved performance improvement due to the multipath propagation and the advantage of using the OFDM signal. We also include the result showing the benefit of using adaptive waveform design. Finally, concluding remarks and some thoughts on a few unaddressed issues are given in Section VI.

II. Problem Description and Modeling

In this section, we first introduce the radar signal model that accounts for the multipath components over multiple frequencies as well as the Doppler shifts. Then, we discuss our statistical assumption on the noise and interference.

A. Target and Environment

We consider a ground moving target in an urban canyon rich in multipath reflections as shown in Fig. 1. At the operating frequency we assume that the building walls only produce specular reflections of the radar signal. We assume that the radar has the complete knowledge of the environment that is under surveillance. Hence, for every range cell it knows

 9781-4244-2971-4/09/$25.00©2009 IEEE

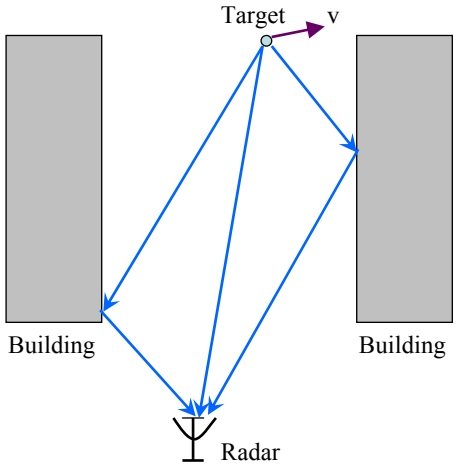

Fig. 1. A schematic representation of the urban scenario.

the number of possible multipath (P) between the radar and the target and the direction-of-arrival (DOA) vectors ($\vec{\boldsymbol{u}}_p$, $p = 1, 2, \ldots, P$) along each such path.

The target is assumed to be in far-field and is moving with a constant velocity $\vec{\boldsymbol{v}}$ relative to the radar. Since P multipath signals impinge on the target from different incident angles, they produce P different relative Doppler shifts $\beta_p = < \vec{\boldsymbol{v}}, \vec{\boldsymbol{u}}_p > /c$, $p = 1, 2, \ldots, P$, where c is the speed of propagation. Here $<, >$ denotes the inner-product operator over the real vector space. Thus, the multipath propagation provides enhanced spatial diversity to our system.

B. Measurement Model

We consider a radar employing OFDM signalling system with L active subcarriers, a bandwidth of B Hz, and pulse duration of T seconds. Let a_l represent the complex weights transmitted over the l-th subcarrier for $l = 1, 2, \ldots, L$. Then, the complex envelope of the received signal corresponding to a specific range cell containing the target is given by

$$y(t) = \sum_{l=1}^{L} \sum_{p=1}^{P} a_l x_{lp} e^{j2\pi(1+\beta_p) l \Delta f (t-\tau_p)} + e(t), \quad \text{for } t = 1, 2, \ldots, N, \tag{1}$$

where x_{lp} is a complex quantity representing the scattering coefficient of the target along l-th subchannel and p-th path, $\Delta f = B/L = 1/T$ denotes the subcarrier spacing, τ_p is the roundtrip delay between the radar and the target along p-th path, $e(t)$ is the additive measurement noise, and N is the number of temporal measurements within a given coherent processing interval (CPI). After demodulation at the output of the l-th subchannel, we get

$$y_l(t) = \sum_{p=1}^{P} a_l x_{lp} e^{jl\omega_p(t-\tau_p)} + e_l(t), \quad \text{for } l = 1, 2, \ldots, L, \ t = 1, 2, \ldots, N, \tag{2}$$

where $\omega_p = 2\pi\beta_p \Delta f$ and $e_l(t)$ is the measurement noise and co-channel interference (CCI) at the l-th subchannel.

In formulating (2) we have implicitly assumed that all the multipath delayed signals from the target lie within the range cell under consideration. We further assume that the relative time gaps between any two multipath signals are very small in comparison with the actual roundtrip delays, i.e., $\tau_1 \approx \tau_2 \approx \cdots \approx \tau_P$. These assumptions can be justified in systems where the path lengths of multipath arrivals differ little (e.g., narrow urban canyon where the range is much greater than the width). Moreover, since the analysis is carried out for a particular range cell, the information of the roundtrip delays are automatically incorporated into the model. Hence, corresponding to a specific range cell containing the target, (3) can be simplified to

$$y_l(t) = \sum_{p=1}^{P} a_l x_{lp} e^{jl\omega_p t} + e_l(t), \quad \text{for } l = 1, 2, \ldots, L, \ t = 1, 2, \ldots, N. \tag{3}$$

Stacking the measurements of all the subchannels into one column vector of dimension $L \times 1$, we get

$$\boldsymbol{y}(t) = \boldsymbol{A}\boldsymbol{X}\boldsymbol{\phi}(t, \boldsymbol{\eta}) + \boldsymbol{e}(t), \quad \text{for } t = 1, 2, \ldots, N, \tag{4}$$

where

- $\boldsymbol{y}(t) = [y_1(t), y_2(t), \ldots, y_L(t)]^T$. Here "$T$" means the transpose operator.
- $\boldsymbol{A} = \text{diag}\{a_1, a_2, \ldots, a_L\}$ is an $L \times L$ complex diagonal matrix that contains the transmitted weights.
- $\boldsymbol{X} = \text{diag}\{\boldsymbol{x}_1, \boldsymbol{x}_2, \ldots, \boldsymbol{x}_L\}$ is an $L \times LP$ complex rectangular block-diagonal matrix where each non-zero block $\boldsymbol{x}_l = [x_{l1}, x_{l2}, \ldots, x_{lP}]$ represents the scattering coefficients of the target at l-th subchannel over all P multipath.
- $\boldsymbol{\phi}(t, \boldsymbol{\eta}) = \left[\boldsymbol{\phi}_1(t, \boldsymbol{\eta})^T, \boldsymbol{\phi}_2(t, \boldsymbol{\eta})^T, \ldots, \boldsymbol{\phi}_L(t, \boldsymbol{\eta})^T\right]^T$ is an $LP \times 1$ complex vector where $\boldsymbol{\phi}_l(t, \boldsymbol{\eta})^T = \left[e^{jl\omega_1 t}, e^{jl\omega_2 t}, \ldots, e^{jl\omega_P t}\right]$ contains the Doppler information of the target at l-th subchannel over all P multipath.
- $\boldsymbol{\eta}$ is a column vector containing the unknown target-velocity components.
- $\boldsymbol{e}(t) = [e_1(t), e_2(t), \ldots, e_L(t)]^T$ is an $L \times 1$ vector of measurement noise and co-channel interference.

Concatenating all the temporal data, defined in (4), into an $L \times N$ matrix we obtain the measurement model as follows:

$$\boldsymbol{Y} = \boldsymbol{A}\boldsymbol{X}\boldsymbol{\Phi}(\boldsymbol{\eta}) + \boldsymbol{E}, \tag{5}$$

where

- $\boldsymbol{Y} = [\boldsymbol{y}(t_1)\, \boldsymbol{y}(t_2)\, \cdots\, \boldsymbol{y}(t_N)]$.
- $\boldsymbol{\Phi}(\boldsymbol{\eta}) = [\boldsymbol{\phi}(t_1, \boldsymbol{\eta})\, \boldsymbol{\phi}(t_2, \boldsymbol{\eta})\, \cdots\, \boldsymbol{\phi}(t_N, \boldsymbol{\eta})]$ is an $LP \times N$ matrix containing the Doppler information of the target through the parameter $\boldsymbol{\eta}$.
- $\boldsymbol{E} = [\boldsymbol{e}(t_1)\, \boldsymbol{e}(t_2)\, \cdots\, \boldsymbol{e}(t_N)]$ is an $L \times N$ matrix comprising measurement noise and interference.

C. Statistical Model

The noise vector $\boldsymbol{e}(t)$ models the measurement noise and co-channel interference at the output of L subchannels. We

assume that $\boldsymbol{e}(t)$ is temporally white and circularly symmetric zero-mean complex Gaussian vector, correlated between different subchannels with unknown positive definite covariance matrix $\boldsymbol{\Sigma}$, i.e., the columns of $\boldsymbol{E}$ are independently and identically distributed according to $\boldsymbol{e}(t) \sim \mathbb{C}\mathcal{N}(\boldsymbol{0}, \boldsymbol{\Sigma})$ for $t = 1, 2, \ldots, N$. This implies that $\boldsymbol{E} \sim \mathbb{C}\mathcal{N}_{L,N}(\boldsymbol{0}, \boldsymbol{I}_N \otimes \boldsymbol{\Sigma})$, where $\boldsymbol{I}_N$ is the identity matrix of dimension N and $\otimes$ represents the Kronecker product. Under this assumption, when the parameter $\boldsymbol{\eta}$ is known, (5) is known as the generalized multivariate analysis of variance (GMANOVA) [6] that has been studied extensively in statistics and applied to a number of applications in signal processing [8].

III. Detection Test

In this section, we first develop a statistical detection test for the model presented in Section II. Our goal is to decide whether a target is present or not in the range cell under consideration. Then we analytically derive the performance characteristics of the test.

We construct the decision problem to choose between two possible hypotheses: the null hypothesis $\mathcal{H}_0$ (target-free hypothesis) or the alternate hypothesis $\mathcal{H}_1$ (target-present hypothesis). This can be expressed as

$$\begin{cases} \mathcal{H}_0: & \boldsymbol{X} = \boldsymbol{0}, \quad \boldsymbol{\Sigma} \text{ unknown} \\ \mathcal{H}_1: & \boldsymbol{X} \neq \boldsymbol{0}, \quad \boldsymbol{\eta}, \boldsymbol{\Sigma} \text{ unknown} \end{cases} \tag{6}$$

It is well known that the optimal detector for this problem is the Neyman-Pearson detector [9] that maximizes the probability of detection (P_{D}) for a certain probability of false alarm (P_{FA}). However, because of the lack of knowledge about $\boldsymbol{\eta}$ and $\boldsymbol{\Sigma}$ we have to use the generalized likelihood ratio (GLR) test in which the unknown parameters are replaced with their maximum likelihood estimates (MLE). Although the GLR test does not have the optimality property, in practice it appears to work quite well. This approach also provides the information about the unknown parameters since the first step is to find the MLEs.

A. GLR Test

When the parameter $\boldsymbol{\eta}$ is known in (5), the GLR test compares the ratio of the likelihood functions under the two hypotheses with a threshold as follows [9, Ch. 6.4.2]:

$$\text{GLR}(\boldsymbol{\eta}) = \frac{f_{\mathcal{H}_1}(\boldsymbol{Y}; \boldsymbol{\eta}, \widehat{\boldsymbol{X}}, \widehat{\boldsymbol{\Sigma}}_1)}{f_{\mathcal{H}_0}(\boldsymbol{Y}; \widehat{\Sigma}_3)} \underset{>}{\overset{\mathcal{H}_1}{}} \gamma, \tag{7}$$

where $f_{\mathcal{H}_0}$ and $f_{\mathcal{H}_1}$ are the likelihood functions under $\mathcal{H}_0$ and $\mathcal{H}_1$, $\widehat{\boldsymbol{\Sigma}}_0$ and $\widehat{\boldsymbol{\Sigma}}_1$ are the MLEs of $\boldsymbol{\Sigma}$ under $\mathcal{H}_0$ and $\mathcal{H}_1$, $\widehat{\boldsymbol{X}}$ is the MLE of $\boldsymbol{X}$ under $\mathcal{H}_1$, and γ is the detection threshold. After some algebraic manipulation, it can be easily shown that the test statistics of this problem is [8]

$$\text{GLR}(\boldsymbol{\eta}) = \frac{\left|\frac{1}{N}\boldsymbol{Y}\boldsymbol{Y}^H\right|}{\left|\frac{1}{N}\left(\boldsymbol{Y} - \boldsymbol{A}\widehat{\boldsymbol{X}}\boldsymbol{\Phi}(\boldsymbol{\eta})\right)\left(\boldsymbol{Y} - \boldsymbol{A}\widehat{\boldsymbol{X}}\boldsymbol{\Phi}(\boldsymbol{\eta})\right)^H\right|}, \tag{8}$$

where $\widehat{\boldsymbol{X}}(\boldsymbol{\eta}) = \left(\boldsymbol{A}^{-1}\boldsymbol{Y}\boldsymbol{\Phi}(\boldsymbol{\eta})^H(\boldsymbol{\Phi}(\boldsymbol{\eta})\boldsymbol{\Phi}(\boldsymbol{\eta})^H)^-\right) \odot \boldsymbol{D}$ and $\boldsymbol{D} = \text{diag}\{\boldsymbol{1}_P\, \boldsymbol{1}_P \cdots \boldsymbol{1}_P\}$ is an $L \times LP$ rectangular block-diagonal matrix where each non-zero block is a P dimensional row vector with all entries equal to 1. Here $|\cdot|$ denotes the determinant operator, "^{H}" is the complex transpose operator, $(\cdot)^-$ represents the generalized inverse of a matrix, and $\odot$ is the element-wise Hadamard product. In case of unknown $\boldsymbol{\eta}$, the GLR test compares $\max_{\boldsymbol{\eta}}\text{GLR}(\boldsymbol{\eta}) = \text{GLR}(\widehat{\boldsymbol{\eta}})$ with a threshold.

B. Detection Performance

When $\boldsymbol{A}$ has full rank L and the matrix $\boldsymbol{X}$ is a full matrix, (8) can be written in a concise form as

$$\frac{1}{\text{GLR}(\boldsymbol{\eta})} = \frac{|\boldsymbol{G}|}{|\boldsymbol{G} + \boldsymbol{H}|}, \tag{9}$$

where $\boldsymbol{G} = \boldsymbol{Y}\boldsymbol{\mathcal{P}}_1\boldsymbol{Y}^H$ and $\boldsymbol{H} = \boldsymbol{Y}\boldsymbol{\mathcal{P}}_2\boldsymbol{Y}^H$. Here $\boldsymbol{\mathcal{P}}_1 = \left[\boldsymbol{I}_N - \boldsymbol{\Pi}\left(\boldsymbol{\Phi}(\boldsymbol{\eta})^H\right)\right]$ and $\boldsymbol{\mathcal{P}}_2 = \boldsymbol{\Pi}\left(\boldsymbol{\Phi}(\boldsymbol{\eta})^H\right) = \boldsymbol{I}_N - \boldsymbol{\mathcal{P}}_1$ are two projection matrices orthogonal to each other and $\boldsymbol{\Pi}\left(\boldsymbol{\Phi}(\boldsymbol{\eta})^H\right)$ is the projection matrix onto the row space of $\boldsymbol{\Phi}(\boldsymbol{\eta})$.

Under $\mathcal{H}_0$ we have $\boldsymbol{Y} \sim \mathbb{C}\mathcal{N}_{L,N}(\boldsymbol{0}, \boldsymbol{I}_N \otimes \boldsymbol{\Sigma})$. Therefore, provided that $(N - r) \geq L$, $\boldsymbol{G} = \boldsymbol{Y}\boldsymbol{\mathcal{P}}_1\boldsymbol{Y}^H$ is distributed as complex Wishart matrix of order L and parameter $\boldsymbol{\Sigma}$ with $(N-r)$ complex degrees of freedom. This is denoted as $\boldsymbol{G} \sim \mathbb{C}\mathcal{W}_L(N-r, \boldsymbol{\Sigma})$. Similarly, we get $\boldsymbol{H} \sim \mathbb{C}\mathcal{W}_L(r, \boldsymbol{\Sigma})$ if $r \geq L$. Here $r = \text{rank}(\boldsymbol{\mathcal{P}}_2) = \text{rank}[\boldsymbol{\Phi}(\boldsymbol{\eta})] \leq LP < N$. Since $\boldsymbol{\mathcal{P}}_1$ and $\boldsymbol{\mathcal{P}}_2$ are orthogonal complement to each other, we get $\boldsymbol{\mathcal{P}}_1\boldsymbol{\mathcal{P}}_2 = \boldsymbol{0}$ and hence, following Craig-Sakamoto theorem [10], [11], $\boldsymbol{G}$ and $\boldsymbol{H}$ are independently distributed. Therefore, the GLR test statistics $1/\text{GLR}(\boldsymbol{\eta})$ is distributed as $\prod_{l=1}^{L} b_l$ [12, Th. 3.10], [13, Eqn. 4-33], where b_l's are mutually independent complex beta distributed random variables with $((N - r) - (L - l))$ and r complex degrees of freedom, written as

$$b_l \sim \mathbb{C}\mathcal{B}((N - r) - (L - l),\, r) \quad \text{for} \quad l = 1, 2, \ldots, L. \tag{10}$$

Note that the expression of the beta distribution does not depend on the unknown covariance matrix $\boldsymbol{\Sigma}$. Thus, when $\boldsymbol{\eta}$ is known, (9) corresponds to a constant false alarm rate (CFAR) test.

However, under $\mathcal{H}_1$ the GLR test statistics does not have a closed-form expression in general. Hence we explore the asymptotic approximations for the distribution of the GLR test statistic. Following an analogous discussion on real Gaussian variables from [14, Ch. 8], we get that as $N \to \infty$, under $\mathcal{H}_0$, $N \ln \text{GLR}(\boldsymbol{\eta})$ has a complex chi-square distribution with Lr complex degrees of freedom. Under $\mathcal{H}_1$, the limiting distribution of $N \ln \text{GLR}(\boldsymbol{\eta})$ is a complex non-central distribution with Lr complex degrees of freedom and non-centrality parameter $\lambda = \sum_{l=1}^{L} \delta_l$, where $\delta_1, \delta_2, \ldots, \delta_L$ are the roots of $\left|\boldsymbol{M}\boldsymbol{M}^H - \delta\widetilde{\boldsymbol{\Sigma}}\right| = 0$ and $\boldsymbol{M} = \boldsymbol{A}\boldsymbol{X}\boldsymbol{\Phi}(\boldsymbol{\eta})$. Obviously another way to represent the same non-centrality parameter is $\lambda = \text{tr}(\widetilde{\boldsymbol{\Sigma}}^{-1}\boldsymbol{M}\boldsymbol{M}^H)$. We may call the matrix $\widetilde{\boldsymbol{\Sigma}}^{-1}\boldsymbol{M}\boldsymbol{M}^H$ as the "signal-to-noise ratio matrix," and hence the trace of it can be considered as a sum of squared Mahalanobis distances [15].

IV. Adaptive Waveform Design

In this section, we develop an adaptive waveform design technique to improve the target-detection performance. To derive a mathematical formulation for optimal waveform selection, we first create a utility function according to certain criteria and then determine the parameters for the next transmitting waveform by maximizing this utility function.

From the discussion of the previous section, we note that when $\boldsymbol{X}$ is a full matrix the GLR test is asymptotically CFAR when $\boldsymbol{\eta}$ is known and the detection performance depends on the system parameters through the non-centrality parameter λ. Although in our problem $\boldsymbol{X}$ is not a full matrix, we maximize the same non-centrality expression with respect to matrix $\boldsymbol{A}$ in order to maximize the probability of detection. Thus, in our optimization approach we aim to achieve

$$\widehat{\boldsymbol{A}} = \underset{\boldsymbol{A}}{\operatorname{argmax}} \left[\operatorname{tr}\left(\boldsymbol{\Sigma}^{-1} \boldsymbol{A}\boldsymbol{X}\boldsymbol{\Phi}\boldsymbol{\Phi}^H \boldsymbol{X}^H \boldsymbol{A}^H \right) - \mu \left(\operatorname{tr}(\boldsymbol{A}\boldsymbol{A}^H) - E_{\boldsymbol{A}} \right) \right], \tag{11}$$

Here we also incorporate a pre-defined energy-constraint on $\boldsymbol{A}$ given by $E_{\boldsymbol{A}}$ and μ denotes the Lagrange multiplier. Note that in a real application the true values of $\boldsymbol{\eta}$, $\boldsymbol{X}$, and $\boldsymbol{\Sigma}_{\mathrm{c}}$ are not known. Hence, their estimates $\widehat{\boldsymbol{\eta}}$, $\widehat{\boldsymbol{X}}$, and $\widehat{\boldsymbol{\Sigma}_{\mathrm{c}}}$ have to be used to obtain the optimal $\boldsymbol{A}$ for the next transmitting pulse based on the current measurements.

V. Numerical Results

We present below the results of several simulations to illustrate our analytical results. The following parameters were common to all of the simulations unless otherwise mentioned.

- We considered an OFDM radar operating with $L = 5$ active subcarriers and the subcarrier spacing of $\Delta f = 20$ MHz.
- The radar aimed to detect a ground moving target in an urban canyon by partitioning the whole surveillance area into several range cells. We simulated the situation of a particular range cell centered at 2 km north and 5m east with respect to the radar.
- We assumed that the target is within this range cell and is moving with velocity $\vec{v} = 10\hat{i} + 10\hat{j}$ m/s.
- The radar received the information of this particular range cell over three different multipaths, i.e., $P = 3$.
- The radar collected $N = 30$ temporal measurements and jointly analyzed them to detect the presence/absence of the target.
- We defined the signal-to-noise ratio as $\mathrm{SNR} = \dfrac{\left[(1/N) \sum_{n=1}^{N} \left(\boldsymbol{A}\boldsymbol{X}\boldsymbol{\phi}(t_n, \boldsymbol{\eta}_{\mathrm{TRUE}}) \right)^H \boldsymbol{A}\boldsymbol{X}\boldsymbol{\phi}(t_n, \boldsymbol{\eta}_{\mathrm{TRUE}}) \right]}{\operatorname{tr}(\boldsymbol{\Sigma})}$, where $\boldsymbol{\eta}_{\mathrm{TRUE}} = [10, 10]^T$.

A. Detector Performance

We performed Monte Carlo simulations based on 10^5 independent trials to characterize the performance of our proposed detector. The entries of $\boldsymbol{X}$ and $\boldsymbol{\Sigma}$ were realized from the $\mathbb{CN}(0, 1)$ distribution and then were scaled to satisfy the required SNR. The matrix $\boldsymbol{A}$ was assumed to be identity matrix. The performance of the detector is analyzed under the following scenarios:

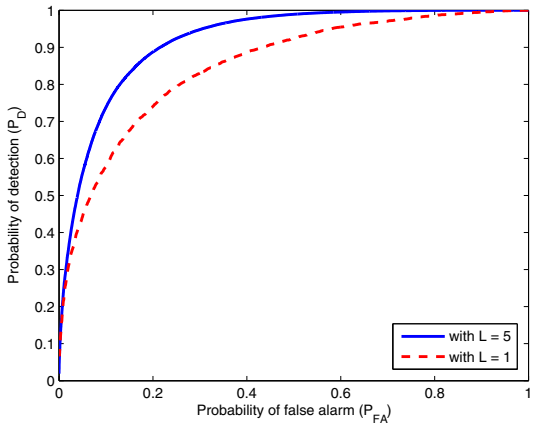

Fig. 2. Probability of detection as a function of probability of false alarm under single-frequency and multi-frequency operations.

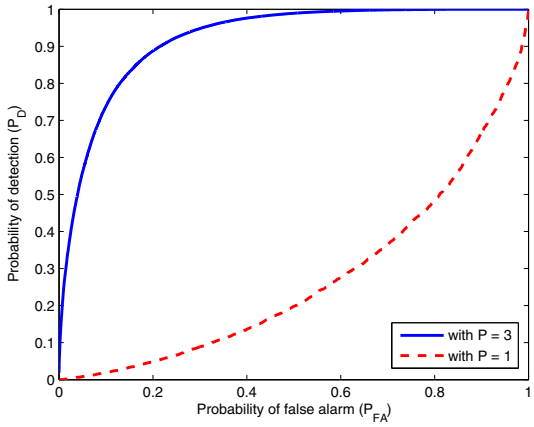

Fig. 3. Probability of detection as a function of probability of false alarm under two different multipath scenarios when the target velocity is perpendicular to the radar line-of-sight.

- To show the advantage of using multi-frequency OFDM signalling system, we compared it with a single-frequency system by keeping the SNR fixed at -5 dB. The result is presented in Fig. 2. Hence, it is evident that the frequency diversity improves the target-detection performance.
- To demonstrate the benefit of exploiting multipath reflections, we modified the target velocity such that it is perpendicular to the radar LOS (which was $5\hat{i}+2000\hat{j}$). Then we compared the situations of having three multipath with that having only one direct path by keeping the SNR fixed at -5 dB. The result is shown in Fig. 3, and hence, it is evident that exploitation multipath components increases the ability of the radar to detect targets.

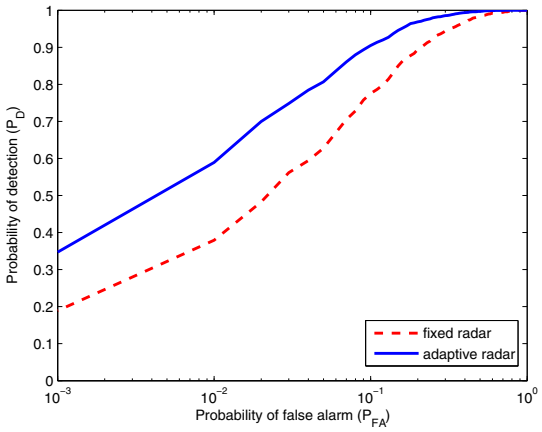

Fig. 4. Improvement on detection probability as a function of probability of false alarm due to the use of adaptive waveform.

B. Adaptive Waveform Design

In Section IV, we proposed an adaptive waveform design technique to improve the target-detection performance. In order to study this improvement we devised a simple problem. We assumed a system in which we transmit $a_l = 1$ for $l = 1, 2, \ldots, L$ in the first CPI, and then based on the corresponding measurements we computed and transmitted the optimized values of a_l's in the next CPI. We compared it with a system in which both the CPIs transmit $a_l = 1$ for $l = 1, 2, \ldots, L$. We fixed the SNR at -5 dB for this simulation. Fig. 4 shows the average detection performance of 50 cases where parameters $\boldsymbol{X}$ and $\boldsymbol{\Sigma}$ were randomly selected. The figure shows the comparative study on the average performance of the conventional system (both the CPIs transmit $a_l = 1 \,\forall\, l$) with that of the adaptive system in which the transmit weights, a_l, in the second CPI were optimally computed in accordance to (11). We observe that the detection performance of the adaptive system is considerably improved. For example, at $P_{\text{FA}} = 10^{-3}$ the adaptive waveform shows an increment in detection probability (P_{D}) from 0.2 to 0.35 with respect to the fixed system.

VI. Conclusions

In this paper, we addressed the problem of detecting a moving target using an OFDM radar and exploiting multipath reflections in an urban canyon. We first developed the measurement model that accounts for the multipath components generated by the specular reflections as well as Doppler shifts. We considered a broadband radar transmitting orthogonal frequency division multiplexing signals. Then, we formulated the detection problem as a hypothesis test to decide about the presence of a moving target. We analyzed the performance of this proposed detector both numerically and analytically. Our numerical results demonstrate the achieved performance improvement due to the multipath propagation in comparison with a single direct path scenario and the advantage of using OFDM signal in comparison with a single frequency operation. Furthermore, based on the analytical performance analysis, we proposed an algorithm to optimally design the parameters for the next transmitting waveform. We presented a numerical example showing the performance improvement that could be obtained due to such adaptive waveform design.

In our future work, we will integrate our detection procedure with a target tracking algorithm in an urban scenario. We will explore other different criteria, e.g., ambiguity function, mutual information, etc., to optimally design the transmit waveform to improve the tracking accuracy. We will also validate the performance of our proposed detector with real data.

References

[1] M. W. Long, *Radar Reflectivity of Land and Sea*, 3rd ed. Dedham, MA: Artech House Publishers, 2001.
[2] A. Pandharipande, "Principles of OFDM," *IEEE Potentials*, vol. 21, no. 2, pp. 16–19, Apr. 2002.
[3] B. L. Floch, R. Halbert-Lassalle, and D. Castelain, "Digital sound broadcasting to mobile receivers," *IEEE Trans. Consum. Electron.*, vol. 35, no. 3, pp. 493–503, Aug. 1989.
[4] G. E. A. Franken, H. Nikookar, and P. V. Genderen, "Doppler tolerance of OFDM-coded radar signals," in *Proc. of the 3rd European Radar Conference*, Manchester, UK, Sep. 13–15, 2006, pp. 108–111.
[5] D. S. Garmatyuk, "Simulated imaging performance of UWB SAR based on OFDM," in *The IEEE 2006 International Conference on Ultra-Wideband*, Sep. 2006, pp. 237–242.
[6] M. S. Srivastava and C. G. Khatri, *An Introduction to Multivariate Statistics*. New York: North-Holland, 1979.
[7] R. F. Potthoff and S. N. Roy, "A generalized multivariate analysis of variance model useful especially for growth curve problems," *Biometrika*, vol. 51, no. 3/4, pp. 313–326, Dec. 1964.
[8] A. Dogandzic and A. Nehorai, "Generalized multivariate analysis of variance: A unified framework for signal processing in correlated noise," *IEEE Signal Process. Mag.*, vol. 20, pp. 39–54, Sep. 2003.
[9] S. M. Kay, *Fundamentals of statistical signal processing: Detection theory*. Upper Saddle River, NJ: Prentice Hall PTR, 1998.
[10] A. T. Craig, "Note on the independence of certain quadratic forms," *The Annals of Mathematical Statistics*, vol. 14, no. 2, pp. 195–197, Jun. 1943.
[11] H. Sakamoto, "On the independence of two statistics," *Res. Mem. Inst. Statist. Math. Tokyo*, vol. 1, no. 9, pp. 1–25, 1944.
[12] H. H. Andersen, M. Højbjerre, D. Sørensen, and P. S. Eriksen, *Linear and Graphical Models for the Multivariate Complex Normal Distribution*. Springer-Verlag, 1995.
[13] E. J. Kelly and K. M. Forsythe, "Adaptive detection and parameter estimation for multidimensional signal models," Lincoln Laboratory, MIT, Lexington, MA, Tech. Rep. 848, Apr. 1989.
[14] T. W. Anderson, *An Introduction to Multivariate Statistical Analysis*, 3rd ed. Hoboken, NJ: John Wiley & Sons, Inc., 2003.
[15] P. C. Mahalanobis, "On the generalized distance in statistics," in *Proc. Nat. Inst. Sciences of India*, vol. 2, 1936, pp. 49–55.